

DOMAIN DECOMPOSITION WITH NONMATCHING GRIDS FOR EXTERIOR TRANSMISSION PROBLEMS VIA FEM AND DTN MAPPING ^{*1)}

Ju-e Yang De-hao Yu

(LSEC, ICMSEC, Academy of Mathematics and Systems Science, Chinese Academy of Sciences,
Beijing 100080, China)

Dedicated to the 70th birthday of Professor Lin Qun

Abstract

In this paper, we are concerned with a non-overlapping domain decomposition method (DDM) for exterior transmission problems in the plane. Based on the natural boundary integral operator, we combine the DDM with a Dirichlet-to-Neumann (DtN) mapping and provide the numerical analysis with nonmatching grids. The weak continuity of the approximation solutions on the interface is imposed by a dual basis multiplier. We show that this multiplier space can generate optimal error estimate and obtain the corresponding rate of convergence. Finally, several numerical examples confirm the theoretical results.

Mathematics subject classification: 65N30, 65N55.

Key words: Domain decomposition, Nature boundary element, Nonmatching grids, Weak continuity, D-N alternating, Dual basis, Projection operator, Error estimate.

1. Introduction

Domain decomposition method (DDM) with nonmatching grids is a kind of nonconforming finite element methods. In the past few years, there is a fast growing interest in this field (see [1], [2], [5], [7]). This kind of DDM allows different discretizations in different nonoverlapping subdomains by some Lagrange multiplier. This nonconforming element method also allows for local refinement in only certain subregions of the computational domain. Hence, it is suitable for parallel computing (see [6]).

The key point to deal with the nonmatching grids is how to choose the matching condition so that the resulting approximation problem possesses the optimal error estimate. The approximate solutions must satisfy some weak continuity such as the integration matching condition, whereas the pointwise matching.

In this paper, we propose a new class of multiplier space for the exterior unbounded problems with annular interfaces, which is based on the idea of dual basis multiplier (refer to [7]). We impose weak continuity conditions in the sense that the jump of the DDM solution across the interface is required to be orthogonal to a space of test functions. Due to the character of annular interface that there is no intersections between any of two subregions, it is easier for us to construct efficient and practical multiplier. The basis functions of the multiplier spaces

* Received March 1, 2006.

¹⁾This work was supported by the National Basic Research Program of China under the grant G19990328, 2005CB321701, and the National Natural Science Foundation of China under the grant 10531080.

are generated by a set of simple functions with local compact supports. The resulting discrete system is still symmetric and positive definite. It will be shown such construction guarantee the optimal energy error estimate for the approximation solutions and the discrete formulation is easy to be solved.

The outline of the paper is as follows. In Section 2, we present the coupled variational formulation for the exterior transmission problem by the finite element method and the natural boundary element method (FEM-NBEM). Then we make a finite element discretization with nonmatching grids for this coupled system in Section 3, and the construction of the multiplier spaces is also introduced. It will be shown that the nonconforming approximation possesses the optimal energy error estimate. In Section 4, we give a D-N alternating method to solve the discrete system and show that this D-N algorithm is convergent and independent of the finite element meshes. Finally, in Section 5, we illustrate these theoretical results by using some numerical examples.

2. FEM-NBEM Coupling

As a model problem, we consider a second order elliptic equation in divergence form coupled with the Laplace equation in the exterior unbounded region. Let Ω_0 be a bounded domain of \mathbb{R}^2 with a Lipschitz-continuous boundary Γ_0 . Ω_1 is the annular region bounded by Γ_0 and another smooth closed curve Γ_1 that is strictly contained in $\mathbb{R}^2 \setminus \bar{\Omega}_0$ (see Figure 1). We denote by Ω_c the complement of $\bar{\Omega}_0 \cup \bar{\Omega}_1$. Assume that $g \in H^{1/2}(\Gamma_0)$ and $f \in L^2(\Omega_1)$, then the exterior transmission problem reads as: find u such that

$$u_1 = g, \quad \text{on } \Gamma_0 \quad -\operatorname{div}(A\nabla u_1) = f \quad \text{in } \Omega_1 \quad (2.1a)$$

$$u_1 = u_c \quad \text{and} \quad (A\nabla u_1) \cdot \mathbf{n} = \frac{\partial u_c}{\partial \mathbf{n}} \quad \text{on } \Gamma_1 \quad (2.1b)$$

$$-\Delta u_c = 0, \quad \text{in } \Omega_c \quad u_c(x) = O(1) \quad \text{as } |x| \rightarrow \infty \quad (2.1c)$$

where $\mathbf{n} = (n_1, n_2)^T$ denotes the unit outward normal to Γ_1 and A is uniformly symmetric pos-

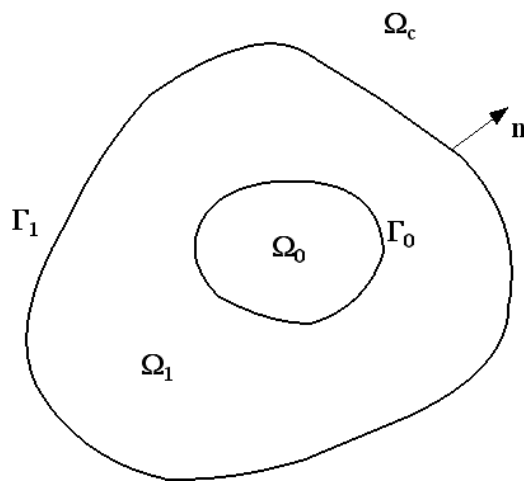


Figure 1: The domain of transmission problem

itive definite matrix with Lipschitz-continuous coefficients, that is to say, there exists constants

α_1 and α_2 such that

$$\alpha_1 \|\boldsymbol{\eta}\|^2 \leq (A\boldsymbol{\eta}) \cdot \boldsymbol{\eta} \leq \alpha_2 \|\boldsymbol{\eta}\|^2 \quad \forall \boldsymbol{\eta} \in \mathbb{R}^2 \tag{2.2}$$

Since Γ_1 is not a circle generally, we draw a auxiliary circle Γ_2 with radius R , centered at the origin, such that its interior region contains $\bar{\Omega}_0 \cup \bar{\Omega}_1$ properly. The auxiliary boundary divides the exterior region of Γ_1 into two nonoverlapping subdomains: one bounded annular domain denoted by Ω_2 , another unbounded subdomain denoted by Ω_3 . Set $\Omega := \Omega_1 \cup \Gamma_1 \cup \Omega_2$, then $\Omega_3 = \mathbb{R}^2 \setminus \bar{\Omega}$, and define $u_i = u|_{\Omega_i}, i = 1, 3$. For the picture see Figure 2.

Define

$$H_{\Gamma_0}^1(\Omega) := \{v \in H^1(\Omega) : v|_{\Gamma_0} = g\} \quad \text{and} \quad H_0^1(\Omega) := \{v \in H^1(\Omega) : v|_{\Gamma_0} = 0\} \tag{2.3}$$

Then we rewrite our exterior transmission (1.1a-1.1c) as follows: Find $u \in H_{\Gamma_0}^1(\Omega)$ such that

$$u_1 = g, \quad \text{on } \Gamma_0 \quad -\operatorname{div}(A\nabla u_1) = f \quad \text{in } \Omega_1 \tag{2.4a}$$

$$u_1 = u_2 \quad \text{and} \quad (A\nabla u_1) \cdot \mathbf{n} = \frac{\partial u_2}{\partial \mathbf{n}} \quad \text{on } \Gamma_1 \tag{2.4b}$$

$$-\Delta u_2 = 0, \quad \text{in } \Omega_2 \tag{2.4c}$$

$$u_2 = u_3, \quad \frac{\partial u_2}{\partial \mathbf{n}} = \frac{\partial u_3}{\partial \mathbf{n}} \quad \text{on } \Gamma_2 \tag{2.4d}$$

$$-\Delta u_3 = 0, \quad \text{in } \Omega_3, \quad u_3(x) = O(1) \quad \text{as } |x| \rightarrow \infty \tag{2.4e}$$

Here we use standard notations for Sobolev spaces and their norms and semi-norms. $(\cdot, \cdot)_{\Omega_i}$,

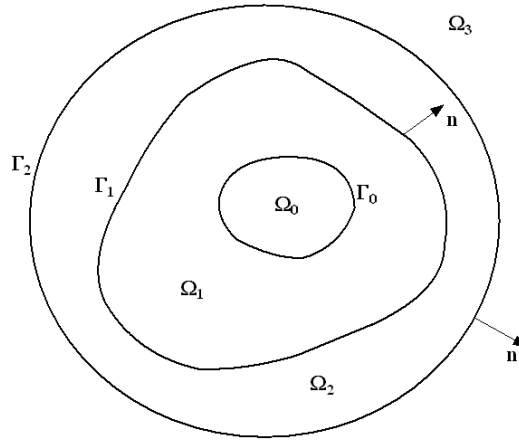


Figure 2: $\Omega = \Omega_1 \cup \Gamma_1 \cup \Omega_2$ and Γ is an auxiliary circle

$\langle \cdot, \cdot \rangle_{\Gamma_i}$ denote the L^2 inner product in Ω_i and on Γ_i , respectively.

Applying the natural boundary reduction principle([10],[11]) in the exterior region Ω_3 , we obtain the Poisson integral formula

$$u(r, \theta) = \frac{r^2 - R^2}{2\pi} \int_0^{2\pi} \frac{\lambda(\theta')}{R^2 + r^2 - 2Rr \cos(\theta - \theta')} d\theta', \quad r > R \tag{2.5}$$

and the natural integral equation

$$\frac{\partial u(\theta)}{\partial \mathbf{n}} = -\frac{1}{4\pi R} \int_0^{2\pi} \frac{\lambda(\theta')}{\sin^2 \frac{\theta-\theta'}{2}} d\theta' = -\frac{1}{4\pi \sin^2 \frac{\theta}{2}} * \lambda(\theta) \quad (2.6)$$

Here $*$ denotes the convolution with respect to θ . Define $\mathcal{K} : H^{1/2}(\Gamma) \rightarrow H^{-1/2}(\Gamma)$ as the natural integral operator, then (2.6) can be written

$$\frac{\partial u(\theta)}{\partial \mathbf{n}} \equiv -\mathcal{K}\lambda(\theta) \quad (2.7)$$

Next, we multiply the divergence partial differential equation in (1.1) by any test function $v \in H_0^1(\Omega)$ and apply the Green formula to yield

$$\int_{\Omega_1} (A\nabla u_1) \cdot \nabla v dx - \int_{\Gamma_1} (A\nabla u_1) \cdot \mathbf{n} v ds = \int_{\Omega_1} f v dx \quad (2.8)$$

According to the interface condition (2.4b), we have

$$\int_{\Omega_1} (A\nabla u_1) \cdot \nabla v dx - \int_{\Gamma_1} \frac{\partial u_2}{\partial \mathbf{n}} v ds = \int_{\Omega_1} f v dx \quad (2.9)$$

In the same way, on Ω_2 , we get

$$\int_{\Omega_2} \nabla u_2 \cdot \nabla v dx + \int_{\Gamma_1} \frac{\partial u_2}{\partial \mathbf{n}} v ds - \int_{\Gamma_2} \frac{\partial u_2}{\partial \mathbf{n}} v ds = 0 \quad (2.10)$$

which, due to the natural integral equation (2.7), becomes

$$\int_{\Omega_2} \nabla u_2 \cdot \nabla v dx + \int_{\Gamma_1} \frac{\partial u_2}{\partial \mathbf{n}} v ds + \int_{\Gamma_2} v \mathcal{K} u_2 ds = 0 \quad (2.11)$$

Adding (2.9) and (2.11), we obtain the coupled FEM-NBEM variational problem of (2.4):

$$\begin{cases} \text{find } u \in H_{\Gamma_0}^1(\Omega) \text{ such that} \\ a(u, v) = f(v), \quad \forall v \in H_0^1. \end{cases} \quad (2.12)$$

where $a(u, v)$ is the bilinear form

$$a(u, v) := (A\nabla u, \nabla v)_{\Omega_1} + (\nabla u, \nabla v)_{\Omega_2} + \langle \mathcal{K}u, v \rangle_{\Gamma_2} \quad (2.13)$$

and $f(v) := (f, v)_{\Omega_1}$ is the linear functional.

Lemma 2.1. *The natural integral operator $\mathcal{K} : H^{\frac{1}{2}}(\Gamma_2) \rightarrow H^{-\frac{1}{2}}(\Gamma_2)$ is just the Dirichlet-Neumann operator (Steklov-Poincaré operator) for the exterior domain Ω_3 . It is symmetric and semi-positive definite with respect to the inner product $\langle \cdot, \cdot \rangle_{\Gamma_2}$, (see [10], [11]), i.e. there is a positive constant c such that*

$$\langle \mathcal{K}v, v \rangle_{\Gamma_2} \geq c \|v\|_{\frac{1}{2}, \Gamma_2}^2, \quad \forall v \in H^{1/2}(\Gamma_2)/P_0 \quad (2.14)$$

where P_0 denotes the set of all constants.

which together with the strongly elliptic condition (2.2) of A , yields the following coercivity lemma.

Lemma 2.2. *Suppose that the matrix valued function A satisfies the condition (2.2). Then, for any function $v \in H_0^1(\Omega)$ there exists a positive constant C such that*

$$a(v, v) \geq C(|v|_{1,\Omega_1}^2 + |v|_{1,\Omega_2}^2 + \|v\|_{\frac{1}{2},\Gamma_2}^2) \tag{2.15}$$

Therefore, the coercivity and the continuity of $a(u, v)$ and the boundedness of $f(v)$ give the uniqueness solvability of the variational problem (2.12) according to the Lax-Milgram Lemma.

3. Finite Element Discretization with Non-matching Grids

In this section, we make a finite element discretization for the subdomains and introduce the non-matching grids method (See [8]) and the construction of basis functions of the Lagrange multiplier space. The main motivation to do this is that we can couple different discretizations in different subdomains in this way. It seems very reasonable especially for the case of singularities of the solution.

Families of finite element triangulations $\mathcal{T}_{h_i}, i = 1, 2$, are associated with Ω_1 and Ω_2 (e.g. some regular quasi-uniform triangles and curved triangles at the interfaces). We denote by h_i the maximum diameter of the elements of \mathcal{T}_{h_i} . But in most real calculation, the curved triangles nearby the interfaces are approximated by the straight triangles which has the same nodes with the curved triangles. This simplified method generates only small error. Let $V_{h_i}(\Omega_i) \subset H^1(\Omega_i), i = 1, 2$, be the finite element spaces on Ω_i with respect to $\mathcal{T}_{h_i}, i = 1, 2$. Next, we discretize the auxiliary circle Γ_2 . Given $n \in \mathbb{N}$, we let $0 = t_0 \leq t_1 \leq \dots \leq t_n = 2\pi$ be a uniform partition of $[0, 2\pi]$ with $h_3 = t_{i+1} - t_i = \frac{2\pi}{n}, j = 0, 1, \dots, n - 1$, which generates a division \mathcal{T}_{h_3} on Γ_2 . We denote this boundary element space by $V_{h_3}(\Gamma_2)$.

The division in $\Omega_i, i = 1, 2$ leads to a division on the interface Γ_1 and Γ_2 , so we set

$$V_{h_i}(\Gamma_1) = \{v|_{\Gamma_1} : v \in V_{h_i}(\Omega_i), i = 1, 2\} \quad \text{and} \quad V_{h_2}(\Gamma_2) = \{v|_{\Gamma_2} : v \in V_{h_2}(\Omega_2)\} \tag{3.1}$$

We note that the meshes need not match at the interface between any two subdomains. Thus in order to discretize the space $H_{\Gamma_0}^1(\Omega)$, we have to introduce a Lagrange multipliers space M_h used to impose a weak continuity constraint across the interface.

We set the product spaces Q_h

$$Q_h := V_{h_1}(\Omega_1) \times V_{h_2}(\Omega_2) \times V_h(\Gamma_2) \tag{3.2}$$

Define

$$V_h = \{v_h = (v_{h_1}, v_{h_2}, v_{h_3}) \in Q_h : \int_{\Gamma_1 \cup \Gamma_2} [v_h] \cdot \mu ds = 0, \forall \mu \in M_h(\Gamma_i), i = 1, 2\}, \tag{3.3}$$

$$V_h^0 = \{v_h \in V_h : v_{h_1}|_{\Gamma_0} = 0\} \tag{3.4}$$

where $[\cdot]$ denotes the jump of the function v_h across the interfaces.

Then we obtain the discrete problem of (2.12) with respect to this kind of non-matching grids discretization.

$$\begin{cases} \text{find } u_h \in V_h \text{ such that} \\ a(u_h, v_h) = f(v_h), \quad \forall v_h \in V_h^0. \end{cases} \tag{3.5}$$

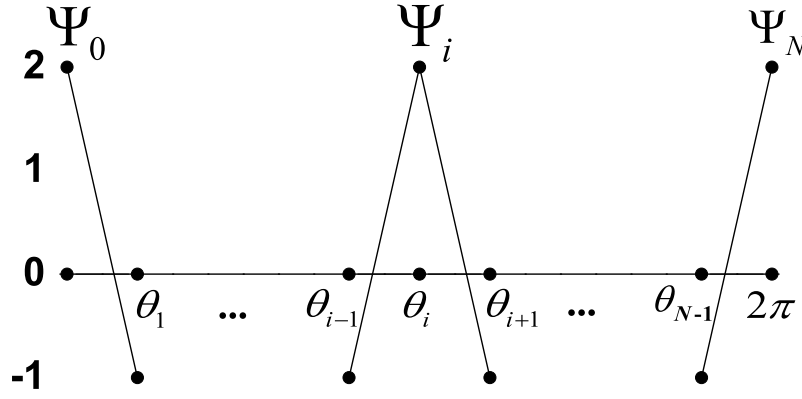


Figure 3: Dual basis functions

Remark 3.1. The setting of Lagrange multipliers space would guarantee uniform ellipticity of this discrete problem(see [8]). Then it can be shown that the coupled discrete problem (3.5) has unique solution $(u_{h_1}, \varphi_{h_2}) \in V_h$.

As we have seen, the construction of Lagrange multiplier space is of great importance for the unique solvability. It is proven in [7] the dual basis mortar method leads to a stable and optimally convergent approximation. Here we apply the same dual basis approach and introduce a new non-matching grids method for unbounded domain problems (see [8]).

Here and below we only discuss the interface Γ_1 . A similar definition is to the interface Γ_2 . To avoid confusion for the subscript, let us denote by $\Gamma = \Gamma_i, i = 1, 2$. Let N be the number of nodes on Γ and $\{a_i\}_{i=1}^N$ be the set of nodal points in Γ . For the nodal basis $\{\Phi_i\}_{i=1}^N$, we define by the dual basis $\{\Psi_i(\theta)\}_{i=1}^N$ (see Figure 3 for piecewise linear basis functions)

$$\langle \Phi_i(\theta), \Psi_j(\theta) \rangle_\Gamma = \delta_{i,j} \langle \Phi_i(\theta), 1 \rangle_\Gamma, \quad 1 \leq i, j \leq N \tag{3.6}$$

where δ_{ij} is the Kronecker symbol.

Before we begin the analysis of error estimate, we will introduce two important projection operator. Since each interface has two sides, we denote by Γ_{12} and Γ_{21} . Define the projection operator Π_h in such way : it maps the space $V_h(\Gamma_{12})$ into $V_h(\Gamma_{21})$ or maps $V_h(\Gamma_{21})$ into $V_h(\Gamma_{12})$. We can see that the choice of side is rather arbitrary. In our case, we choose the fine mesh side as the beginning such as Γ_{12} . That is to say, Given $v \in L^2(\Gamma)$, the values of $\Pi_h v \in V_h(\Gamma_{21})$ can be determined by

$$\int_\Gamma (v - \Pi_h v) \mu ds = 0, \quad \forall \mu \in M_h(\Gamma). \tag{3.7}$$

Since $V_{h_i}(\Gamma) \subset H^{\frac{1}{2}}(\Gamma)$, the multiplier space $M_h(\Gamma)$ generated by the dual basis may be embedded in the dual space of $H^{\frac{1}{2}}(\Gamma)$ with respect to the L^2 -inner product. Therefore, $M_h(\Gamma) \subset H^{-\frac{1}{2}}(\Gamma)$. This operator was used in ([2],[7],[8]) and plays a central role in the error analysis of the nonmatching grid finite discretization.

Then define by $P_h : L^2(\Gamma) \rightarrow M_h(\Gamma)$ the usual orthogonal projection operator. We recall its approximation properties in the following lemma. We can verify it in the standard manner and do not include the proof here. See the proof in [7].

Lemma 3.1. *For any real number s , $0 \leq s \leq 1$, there exist constants such that the following estimates hold for any function v in $H^s(\Gamma)$:*

$$\|v - P_h v\|_{0,\Gamma} \leq c h^s \|v\|_{s,\Gamma}, \quad (3.8)$$

$$\|v - P_h v\|_{(H^{\frac{1}{2}}(\Gamma))'} \leq c h^{s+\frac{1}{2}} \|v\|_{s,\Gamma}. \quad (3.9)$$

Here the dual norm is defined by

$$\|f\|_{X'} := \sup_{v \in X} \frac{\langle f, v \rangle}{\|v\|_X}, \quad (3.10)$$

where X' is the dual space of the Hilbert space X . The definition of operator P_h yields to:

$$\int_{\Gamma} (v - P_h v) \mu ds = 0, \quad \forall \mu \in M_h(\Gamma), \quad (3.11)$$

where $P_h v \in M_h(\Gamma)$. Then

$$\int_{\Gamma} (\Pi_h v - P_h v) \mu ds = 0 \quad \forall \mu \in M_h(\Gamma), \quad (3.12)$$

which means $P_h v$ is also the projection of $\Pi_h v$ into the multiplier space $M_h(\Gamma)$.

The next lemma shows the stability property of the projection operator Π_h in $L^2(\Gamma)$ and $H^1(\Gamma)$.

Lemma 3.2. *There exist a constant $c > 0$ such that for $\forall v \in L^2(\Gamma)$*

$$\|\Pi_h v\|_{0,\Gamma} \leq c \|v\|_{0,\Gamma}, \quad (3.13)$$

Let $v \in H^1(\Gamma)$, then for uniform meshes we have

$$\|\Pi_h v\|_{1,\Gamma} \leq c' \|v\|_{1,\Gamma}. \quad (3.14)$$

Proof. For any $v \in L^2(\Gamma)$, $\Pi_h v$ can be written as

$$\Pi_h v = \sum_{i=1}^N \alpha_i \Phi_i(\theta), \quad (3.15)$$

Substitute $\Pi_h v$ for (3.15) in (3.7). Due to the global orthogonality relation (3.6) between the nodal basis $\{\Phi_i\}$ and its dual basis $\{\Psi_i\}$, the values of α_i can be direct calculated by the formula

$$\alpha_i = \Pi_h v(a_i) = \frac{\int_{\Gamma} v|_{\Omega_1} \Psi_i ds}{\int_{\Gamma} \Phi_i ds}. \quad (3.16)$$

Then some primary inequalities lead to

$$\begin{aligned} \|\Pi_h v\|_{0,\Gamma}^2 &\leq \sum_{i=1}^n \int_{\Gamma} (\Pi_h v(a_i))^2 \Phi_i^2 ds \\ &\leq \sum_{i=1}^n \frac{\int_{\Gamma} \Phi_i^2 ds \int_{\Gamma} \Psi_i^2 ds}{(\int_{\Gamma} \Phi_i ds)^2} \|v\|_{0,\gamma}^2 \leq c \|v\|_{0,\Gamma}^2, \end{aligned} \quad (3.17)$$

in which γ denotes $\overline{\text{supp}\Phi_i}$ and c is a constant. Thus, (3.13) is obtained.

Let $0 = a_0 \leq a_1 \leq \dots \leq a_N = 2\pi$ be a corresponding uniform partition on Γ , which generates a division \mathcal{T}_h for the interface Γ . Let \hat{T} be the 1-dimensional reference element. Let $\{\hat{\phi}_i\}$ be a nodal basis for \hat{T} and let $\{\hat{\psi}_i\}$ be the dual basis with respect to the inner product for $L^2(\hat{T})$.

In order to derive the stability in $H^1(\Gamma)$, we introduce the piecewise affine mapping

$$F(\hat{\theta}) = \beta \hat{\theta} + \theta_0, \quad (3.18)$$

which maps \hat{T} one-to-one and onto some $T \in T_i = [a_{i-1}, a_i]$. Let $\{\hat{\phi}_i\}$ be the nodal basis for \hat{T} and let $\{\hat{\psi}_i\}$ be the dual basis with respect to the inner product for $L^2(\hat{T})$. Then we have (see [3]), for any $v \in H^1(T)$,

$$\|v\|_{1,T} \leq h^{-\frac{1}{2}} \|\hat{v}\|_{1,\hat{T}}, \quad (3.19)$$

$$\|v\|_{L^1(T)} \leq h \|\hat{v}\|_{L^1(\hat{T})} \leq h \|\hat{v}\|_{1,\hat{T}} \leq (h^{\frac{1}{2}} |v|_{0,T} + h^{\frac{3}{2}} |v|_{1,T}), \quad (3.20)$$

here, $h := \max_{T \in \mathcal{T}_h} \text{diam}(T)$.

For any $v \in H^1(\Gamma)$, we can prove the local estimat

$$\begin{aligned} \|\Pi_h v\|_{1,T} &\leq \sum_{i=1}^k |\Pi_h v(a_i)| \|\phi_i\|_{1,T} \leq Ch^{-\frac{1}{2}} \max_{1 \leq i \leq n} \|\hat{\phi}_i\|_{1,\hat{T}} \sum_{i=1}^k |\Pi_h v(a_i)| \\ &\leq h^{-\frac{1}{2}} \sum_{i=1}^k \left| \frac{\int_T \psi_i v ds}{\int_T \phi_i ds} \right| \leq Ch^{-\frac{1}{2}} \sum_{i=1}^k \|\psi_i\|_{L^\infty(T)} \|v\|_{L^1(T)} \\ &\leq Ch^{-\frac{1}{2}} h^{-1} (h^{\frac{1}{2}} |v|_{0,T} + h^{\frac{3}{2}} |v|_{1,T}) \\ &\leq C(h^{-1} |v|_{0,T} + |v|_{1,T}), \end{aligned} \quad (3.21)$$

where ϕ_i and ψ_i are the nodal basis and dual basis for T_i . The global estimate (3.14) is obtained by summing over all local contributions.

Then, by an interpolation argument, the following estimate holds for any function v in $H^{\frac{1}{2}}(\Gamma)$:

$$\|\Pi_h v\|_{\frac{1}{2},\Gamma} \leq C \|v\|_{\frac{1}{2},\Gamma}. \quad (3.22)$$

Define the norm

$$\|v_h\| = \left(\|v_{h_1}\|_{1,\Omega_1}^2 + \|v_{h_2}\|_{1,\Omega_2}^2 + \|v_{h_3}\|_{\frac{1}{2},\Gamma}^2 \right)^{1/2}. \quad (3.23)$$

For our nonconforming situation we use the well-known second Strang's lemma. Let $u = (u_1, u_2, \lambda)$ and $u_h = (u_{h_1}, u_{h_2}, \lambda_{h_3})$ be the solutions of (2.4) and (3.5), respectively. The error can be formulated as follows:

$$\|u - u_h\| \leq \inf_{v_h \in V_h^0} \|u - v_h\| + \sup_{0 \neq v_h \in V_h^0} \frac{\int_{\Gamma_1 \cup \Gamma_2} \frac{\partial u}{\partial \mathbf{n}} [v_h] ds}{\|v_h\|}. \quad (3.24)$$

where $v_h = (v_{h_1}, v_{h_2}, v_{h_3})$. We note that the first term of the right hand of (3.24) is the approximation error, while the second term is the consistency error. The best approximation error can be estimated by using interpolation inequalities for conforming finite elements and stability properties of the projection Π_h ; For estimation of the consistency error, we use the fact

the jump of the solution is orthogonal to the multiplier space M_h . We summarize the results in the following lemmas.

Lemma 3.3. *Assume that the solution u of problem 2.4 is satisfy, for any real number s , $\frac{1}{2} \leq \varepsilon_i \leq 1, i = 1, 2$, $u|_{\Omega_1} \in H^{1+\varepsilon_1}(\Omega_1)$, $u|_{\Omega_2} \in H^{1+\varepsilon_2}(\Omega_2)$ and $u|_{\Gamma_2} \in H^{\frac{3}{2}}(\Gamma_2)$. Then there exists a function $v_h \in V_h^0$ such that*

$$\|u - v_h\| \leq C(h_1^{\varepsilon_1} \|u\|_{1+\varepsilon_1, \Omega_1} + h_2^{\varepsilon_2} \|u\|_{1+\varepsilon_2, \Omega_2} + h_3 \|u\|_{\frac{3}{2}, \Gamma_2}). \quad (3.25)$$

Proof. First, we estimate the error bound on Γ_1 . Let $\pi_{h_i}, i = 1, 2$ are the Lagrange interpolation operators in $\Omega_i, i = 1, 2$, respectively. Then we define v_h by

$$v_{h_1} = \pi_{h_1} u_1, \quad v_{h_2} = \pi_{h_2} u_2 + \Pi_h[\pi_{h_1}(u_1|_{\Gamma_1}) - \pi_{h_2}(u_2|_{\Gamma_1})]. \quad (3.26)$$

In this way, recalling the definition of projection Π_h , we have

$$\begin{aligned} \langle v_{h_1} - v_{h_2}, \mu \rangle_{\Gamma_1} &= \langle \{\pi_{h_1}(u_1|_{\Gamma_1}) - \pi_{h_2}(u_2|_{\Gamma_1})\} - \Pi_h\{\pi_{h_1}(u_1|_{\Gamma_1}) - \pi_{h_2}(u_2|_{\Gamma_1})\}, \mu \rangle_{\Gamma_1} \\ &= 0. \end{aligned} \quad (3.27)$$

For the interface Γ_2 , we also define

$$v_{h_2} = \pi_{h_2} u_2, \quad v_{h_3} = \pi_{h_3} \lambda + \Pi_h[\pi_{h_2}(u_2|_{\Gamma_2}) - \pi_{h_3} \lambda], \quad (3.28)$$

where π_{h_3} is the usual Lagrange interpolation operators on Γ_2 .

Then the trace theorem and the stability properties of Π_h lead to

$$\begin{aligned} \inf_{v_h \in V_h^0} \|u - v_h\| &\leq \inf_{v_h \in V_h^0} \left(\|u_1 - v_{h_1}\|_{1, \Omega_1} + \|u_2 - v_{h_2}\|_{1, \Omega_2} + \|\lambda - v_{h_3}\|_{\frac{1}{2}, \Gamma_2} \right) \\ &\leq \|u - \pi_{h_1} u\|_{1, \Omega_1} + \|u - \pi_{h_2} u\|_{1, \Omega_2} + \|u - \pi_{h_3} u\|_{\frac{1}{2}, \Gamma_2} \\ &\quad + \|\Pi_h(\pi_{h_1} u_1 - \pi_{h_2} u_2)\|_{\frac{1}{2}, \Gamma_1} + \|\Pi_h(\pi_{h_2} u_2 - \pi_{h_3} \lambda)\|_{\frac{1}{2}, \Gamma_2} \\ &\leq ch_1^{\varepsilon_1} \|u_1\|_{1+\varepsilon_1, \Omega_1} + ch_2^{\varepsilon_2} \|u_2\|_{1+\varepsilon_2, \Omega_2} + ch_3 \|\lambda\|_{\frac{3}{2}, \Gamma_2}, \end{aligned} \quad (3.29)$$

which complete the proof.

Lemma 3.4. *Assume that the solution u of problem 2.4 satisfies the same regularity conditions as the lemma 3.3. then there exists a function $v_h \in V_h^0$ such that*

$$\sup_{0 \neq v_h \in V_h^0} \frac{\int_{\Gamma_1 \cup \Gamma_2} \frac{\partial u}{\partial \mathbf{n}} [v_h] ds}{\|v_h\|} \leq C(h_1^{\varepsilon_1} \|u\|_{1+\varepsilon_1, \Omega_1} + h_3 \|u\|_{\frac{3}{2}, \Gamma_2}). \quad (3.30)$$

Proof. First, we fix our attention to the error on Γ_1 . From (3.24) and by using the definition

of the projection operators P_h and Π_h , we have

$$\begin{aligned} \left| \int_{\Gamma_1} \frac{\partial u}{\partial \mathbf{n}} [v_h] ds \right| &= \left| \int_{\Gamma_1} \frac{\partial u}{\partial \mathbf{n}} (v_{h_1} - \Pi_h v_{h_1}) ds \right| \\ &= \left| \int_{\Gamma_1} \left(\frac{\partial u}{\partial \mathbf{n}} - P_h \frac{\partial u}{\partial \mathbf{n}} \right) (v_{h_1} - \Pi_h v_{h_1}) ds \right| \\ &\leq \left\| \frac{\partial u}{\partial \mathbf{n}} - P_h \frac{\partial u}{\partial \mathbf{n}} \right\|_{-\frac{1}{2}, \Gamma_1} \|v_{h_1} - \Pi_h v_{h_1}\|_{\frac{1}{2}, \Gamma_1} \\ &\leq \left\| \frac{\partial u}{\partial \mathbf{n}} - P_h \frac{\partial u}{\partial \mathbf{n}} \right\|_{-\frac{1}{2}, \Gamma_1} \left(\|v_{h_1}\|_{\frac{1}{2}, \Gamma_1} + \|v_{h_2}\|_{\frac{1}{2}, \Gamma_1} \right). \end{aligned} \tag{3.31}$$

Applying the lemma 3.1 and the trace theorem for v_{h_i} we deduce that

$$\begin{aligned} \left| \int_{\Gamma_1} \frac{\partial u}{\partial \mathbf{n}} [v_h] ds \right| &\leq Ch_1^{\varepsilon_1} \left\| \frac{\partial u}{\partial \mathbf{n}} \right\|_{\frac{1}{2} + \varepsilon_1} (\|v_{h_1}\|_{1, \Omega_1} + \|v_{h_2}\|_{1, \Omega_2}) \\ &\leq Ch_1^{\varepsilon_1} \|u\|_{1 + \varepsilon_1, \Omega_1} (\|v_{h_1}\|_{1, \Omega_1} + \|v_{h_2}\|_{1, \Omega_2}). \end{aligned} \tag{3.32}$$

The error bound on Γ_2 can be found in [8]:

$$\left| \int_{\Gamma_2} \frac{\partial u}{\partial \mathbf{n}} [v_h] ds \right| \leq Ch_3 \|u\|_{\frac{3}{2}, \Gamma_2} \left(\|v_{h_2}\|_{1, \Omega_2} + \|v_{h_3}\|_{\frac{1}{2}, \Gamma_2} \right). \tag{3.33}$$

Combining (3.32) and (3.33), we obtain (3.30).

The following theorem conclude the discrete error analysis. We can see that the weak constraint across the interfaces we have defined, for the circle interface, is sufficient to guarantee the optimal error estimate.

Theorem 3.1. *Assume that the solution u of problem 2.4 have the same regularity as the lemma 3.4 and lemma 3.3, then the exact solution u of (2.4) and the approximate solution u_h of (3.5) satisfy*

$$\|u - u_h\| \leq C(h_1^{\varepsilon_1} \|u\|_{1 + \varepsilon_1, \Omega_1} + h_2^{\varepsilon_2} \|u\|_{1 + \varepsilon_2, \Omega_2} + h_3 \|u\|_{\frac{3}{2}, \Gamma_2}). \tag{3.34}$$

where $C > 0$ is a constant independent of the mesh parameters $h_i, i = 1, 3$.

Remark 3.2. In order to obtain the optimal error estimation in V_h^0 , we should balance the finite element grids in $\Omega_i, i = 1, 3$ such that the fine mesh size $h_i, i = 1, 3$ satisfy $h_1^{\varepsilon_1} \approx h_2^{\varepsilon_2} \approx h_3$. The main results given in above theorem can be extended to multi-sub-domains case for the exterior problems.

4. D-N Alternating Method

The exterior transmission problem (2.4) can be solved by a D-N alternating scheme as follows:

1. Choose initial value $\lambda^0 \in H^{\frac{1}{2}}(\Gamma_2)$, $\lambda_1^0 \in H^{\frac{1}{2}}(\Gamma_1)$ and set $n := 0$.

2. Solve the Dirichlet problem on the exterior subdomain Ω_3 :

$$\begin{cases} -\Delta u_3^n = 0 & \text{in } \Omega_3, \\ u_3^n = \Pi_h \lambda^n & \text{on } \Gamma_2, \\ u_3^n = O(1) & \text{as } |x| \rightarrow \infty. \end{cases} \quad (4.1)$$

3. Solve the mixed boundary value problem in the annular subdomain Ω_2 :

$$\begin{cases} -\Delta u_2^n = 0 & \text{in } \Omega_2, \\ \frac{\partial u_2^n}{\partial \mathbf{n}} = \frac{\partial u_3^n}{\partial \mathbf{n}} & \text{on } \Gamma_2, \\ u_2^n = \Pi_h \lambda_1^n & \text{on } \Gamma_1. \end{cases} \quad (4.2)$$

4. Solve nonhomogeneous boundary value problem in the annular subdomain Ω_1 :

$$\begin{cases} -\operatorname{div}(A \nabla u_1^n) = f & \text{in } \Omega_1, \\ (A \nabla u_1^n) \cdot \mathbf{n} = \frac{\partial u_2^n}{\partial \bar{\mathbf{n}}} & \text{on } \Gamma_1, \\ u_1^n = g & \text{on } \Gamma_0. \end{cases} \quad (4.3)$$

5. Let θ_n be the n -th linear relaxation factor selected in computation. Set

$$\lambda^{n+1} = \theta_n u_2^n + (1 - \theta_n) \lambda^n, \quad \text{on } \Gamma_2, \quad (4.4)$$

and

$$\lambda_1^{n+1} = \theta_n u_1^n + (1 - \theta_n) \lambda_1^n, \quad \text{on } \Gamma_1. \quad (4.5)$$

6. Set $n := n + 1$, then goto the second step.

Note that only the approximation of the normal derivative of u_3^n on the interface Γ_2 is required for solving the mixed boundary value problem in the annular subdomain Ω_2 . Thus, in practical computation, it is not necessary to actually solve the Dirichlet problem (4.1). Applying the natural integral equation (2.7) and the projection operator Π_h defined in previous section, we can directly compute the value of $\frac{\partial u_3^n}{\partial \mathbf{n}}$ on Γ_2 :

$$\frac{\partial u_3^n}{\partial \mathbf{n}} = -\mathcal{K}(\Pi_h u_2^n). \quad (4.6)$$

And then through the second and third equation of (4.3), we can solve the PDE system of (4.3) in subdomain Ω_1 .

For the analysis of the convergence of our D-N alternating algorithm, we divide it into two parts. The first part is discussed between the unbounded subdomain Ω_3 and the annular subdomain Ω_2 (see [8]).

Define

$$\begin{aligned} R_1 : H^{1/2}(\Gamma_1) &\rightarrow H^1(\Omega_1), \\ \phi &\mapsto R_1 \phi, \end{aligned}$$

It follows that for any $\phi \in H^{1/2}(\Gamma_1)$, if $w = R_1\phi$, then $w \in H^1(\Omega_1)$ and satisfies

$$\begin{cases} -\operatorname{div}(A\nabla w) = 0, & \text{in } \Omega_1, \\ w = \phi, & \text{on } \Gamma_1, \\ w = 0, & \text{on } \Gamma_0. \end{cases} \quad (4.7)$$

$$\begin{aligned} R_2 : H^{1/2}(\Gamma_1) &\rightarrow H^1(\Omega_2), \\ \phi &\mapsto R_2\phi, \end{aligned}$$

for any $\phi \in H^{1/2}(\Gamma_1)$, if $w = R_2\phi$, then $w \in H^1(\Omega_2)$ and satisfies

$$\begin{cases} -\Delta w = 0, & \text{in } \Omega_2, \\ w = \phi, & \text{on } \Gamma_1, \\ w = 0, & \text{on } \Gamma_2. \end{cases} \quad (4.8)$$

Assume that u_1, u_2 satisfy

$$\begin{cases} -\operatorname{div}(A\nabla u_1) = f, & \text{in } \Omega_1, \\ u_1 = \lambda, & \text{on } \Gamma_1, \\ u_1 = g, & \text{on } \Gamma_0. \end{cases} \quad (4.9)$$

$$\begin{cases} -\Delta u_2 = 0, & \text{in } \Omega_2, \\ u_2 = \Pi_h \lambda, & \text{on } \Gamma_1, \\ u_2 = g_2, & \text{on } \Gamma_2. \end{cases} \quad (4.10)$$

and Q_1, Q_2 satisfy

$$\begin{cases} -\operatorname{div}(A\nabla Q_1) = 0, & \text{in } \Omega_1, \\ Q_1 = 0, & \text{on } \Gamma_1, \\ Q_1 = g, & \text{on } \Gamma_0. \end{cases} \quad (4.11)$$

$$\begin{cases} -\Delta Q_2 = 0, & \text{in } \Omega_2, \\ Q_2 = 0, & \text{on } \Gamma_1, \\ Q_2 = g_2, & \text{on } \Gamma_2. \end{cases} \quad (4.12)$$

Then it's easy to see

$$u_1 = R_1\lambda + Q_1, \quad u_2 = R_2\Pi_h\lambda + Q_2. \quad (4.13)$$

On the interface Γ_1 , λ should satisfies

$$A\nabla u_1(\lambda) \cdot \mathbf{n} = \nabla u_2(\lambda) \cdot \mathbf{n}. \quad (4.14)$$

Set

$$S_1 = -((n_x a_{11} + n_x a_{12}) \frac{\partial}{\partial x}(R_1 \cdot) + (n_y a_{21} + n_y a_{22}) \frac{\partial}{\partial y}(R_1 \cdot)), \quad (4.15)$$

$$S_2 = \frac{\partial}{\partial \mathbf{n}}(R_2 \Pi_h \cdot), \quad (4.16)$$

where the coefficients $a_{11}, a_{12}, a_{21}, a_{22}$ are the elements of the matrix function A . Let $S = S_1 + S_2$. Then we obtain the interface equation

$$S\lambda = \chi. \tag{4.17}$$

here S is just the Steklov-Poincaré operator on the interface Γ_1 and χ is independent of λ_1 and can be solved beforehand in the subdomains.

Theorem 4.1. *The D-N alternating method is equivalent to the preconditioned Richardson iterative method*

$$S_1(\lambda^{n+1} - \lambda^n) = \theta_n(\chi - S\lambda^n). \tag{4.18}$$

Proof. We consider the error $e_k^n = u - u_k^n$, $k = 1, 2$ and $\mu^n = \Pi_h(\lambda - \lambda^n)$, where $\lambda = u|_{\Gamma_1}$. Then the error terms e_1^n and e_2^n satisfy the following equations, respectively,

$$\begin{cases} -\Delta e_2^n = 0, & \text{in } \Omega_2, \\ e_2^n = \mu^n, & \text{on } \Gamma_1, \\ e_2^n = 0, & \text{on } \Gamma_2, \end{cases} \tag{4.19a}$$

$$\begin{cases} -\operatorname{div}(Ae_1^n) = 0, & \text{in } \Omega_1 \\ e_1^n = 0, & \text{on } \Gamma_0 \\ \frac{\partial e_1^n}{\partial \mathbf{n}} = -\mathcal{K}(\mu^n), & \text{on } \Gamma_1, \end{cases} \tag{4.19b}$$

and

$$\mu^{n+1} = \theta_n \Pi_h(e_1^n|_{\Gamma_1}) + (1 - \theta_n)\mu^n. \tag{4.20}$$

Therefore,

$$e_1^n = R_1(e_1^n|_{\Gamma_1}), \quad e_2^n = R_2(e_2^n|_{\Gamma_1}) = R_2\mu^n, \tag{4.21}$$

Then we have

$$S_1(e_1^n|_{\Gamma_1}) = -\frac{\partial}{\partial \mathbf{n}}[R_1(e_1^n|_{\Gamma_1})] = \mathcal{K}(\mu^n) = -\frac{\partial}{\partial \mathbf{n}}[\Pi_h(\lambda - \lambda^n)] = -S_2(\lambda - \lambda^n). \tag{4.22}$$

Since

$$\lambda^{n+1} - \lambda^n = \theta_n(u_1^n|_{\Gamma_1} - \lambda^n), \tag{4.23}$$

finally we derive

$$\begin{aligned} S_1(\lambda^{n+1} - \lambda^n) &= S_1[\theta_n(u_1^n|_{\Gamma_1} - \lambda^n)] = \theta_n[S_1(u_1^n|_{\Gamma_1} - \lambda) + S_1(\lambda - \lambda^n)] \\ &= \theta_n(S_1 + S_2)(\lambda - \lambda^n) = \theta_n S(\lambda - \lambda^n) = \theta_n(\chi - S\lambda^n). \end{aligned} \tag{4.24}$$

The proof is completed.

Define by $R_h^i : H^{1/2}(\Gamma_1) \rightarrow V_{h_i}(\Omega_i)$ the discrete harmonic extension operators, i.e. for any $\lambda_h \in H^{1/2}(\Gamma_1)$, $R_h^i \lambda_h \in V_{h_i}(\Omega_i)$ satisfies

$$\begin{cases} a_i(R_h^i \lambda_h, v_h) = 0, & \forall v_h \in V_{h_i}(\Omega_i), \\ R_h^i \lambda_h = \lambda_h, & \text{on } \Gamma_1, \\ R_h^i \lambda_h = 0, & \text{on } \partial\Omega_i \setminus \Gamma_1, \end{cases} \quad i = 1, 2, \tag{4.25}$$

where $a_i(u, v)$, $i = 1, 2$, are the bilinear forms corresponding to the harmonic problems in Ω_i .

The discrete scheme of the D-N alternating methods is as follows:

1. Choose an initial value $\lambda_h^0 \in V_{h_2}(\Gamma_2)$, $\lambda_{1h}^0 \in V_{h_1}(\Gamma_1)$ and set $n := 0$.
2. Apply the natural integral equation on Γ_2 and compute:

$$\frac{\partial u_{h_3}^n}{\partial \mathbf{n}} = -\mathcal{K}\Pi_h \lambda_h^n, \quad \text{on } \Gamma_2. \quad (4.26)$$

3. Solve the discrete mixed boundary value problem in Ω_2 :

$$\left\{ \begin{array}{l} \text{find } u_{h_2} \in V_{h_2}(\Omega_2) \text{ such that } \forall v_{h_2} \in V_{h_2}(\Omega_2), \\ \int_{\Omega_2} \nabla u_{h_2}^n \cdot \nabla v_{h_2} dx = \int_{\Gamma_2} \frac{\partial u_{h_3}^n}{\partial \mathbf{n}} \Pi_h v_{h_2} ds + \int_{\Omega_2} \nabla R_h^2 \Pi_h \lambda_{1h}^n \cdot \nabla v_{h_2} ds, \\ u_{h_2}^n = \Pi_h \lambda_{1h}^n \quad \text{on } \Gamma_1. \end{array} \right. \quad (4.27)$$

4. Solve the discrete mixed boundary value problem in Ω_1 :

$$\left\{ \begin{array}{l} \text{find } u_{h_1} \in V_{h_1}(\Omega_1) \text{ such that } \forall v_{h_1} \in V_{h_1}(\Omega_1), \\ \int_{\Omega_1} A \nabla u_{h_1}^n \cdot \nabla v_{h_1} dx = \int_{\Omega_1} f v_{h_1} dx + \int_{\Gamma_1} \Pi_h v_{h_1} \frac{\partial}{\partial \mathbf{n}} u_{h_2}^n ds. \end{array} \right. \quad (4.28)$$

5. Set $\lambda_h^{n+1} = \theta_n u_{h_1}^n + (1 - \theta_n) \lambda_h^n$ on Γ_2 , and $\lambda_{1h}^{n+1} = \theta_n u_{h_1}^n + (1 - \theta_n) \lambda_{1h}^n$ on Γ_1 ,
6. Let $n := n + 1$, then goto the second step.

Theorem 4.2. *The discrete D-N alternating method is equivalent to the associated preconditioned Richardson iterative method*

$$S_h^1(\lambda_h^{n+1} - \lambda_h^n) = \theta_n(\chi - S_h \lambda_h^n), \quad (4.29)$$

and converges if $0 < \theta_n < 1$, where θ_n is the n -th relaxation factor in the computations.

The proof is similar to [8].

5. Numerical Experiments

We now provide some numerical examples to illustrate the theoretical results in precious sections. We use the D-N alternating method to solve the discrete problem (3.5).

Example 1. The solution domain and the triangular mesh are illustrated in Figure 4. In this example we consider A equals the identity matrix I . The exact solution of the problem (2.4) is given by

$$u_1(x, y) = \frac{1}{x^2 + y^2}, \quad u_2(x, y) = \frac{x}{x^2 + y^2} \quad (5.1)$$

with

$$f(x, y) = -\frac{4}{(x^2 + y^2)^2}, \quad (5.2)$$

and the boundary value g on Γ_0 is computed from the exact solution $u_1|_{\Gamma_0}$.

The discrete system (3.5) is solved by the D-N alternating method proposed in Section 4. In our computation we compute the natural boundary element matrix \mathbf{K} , and then solve the

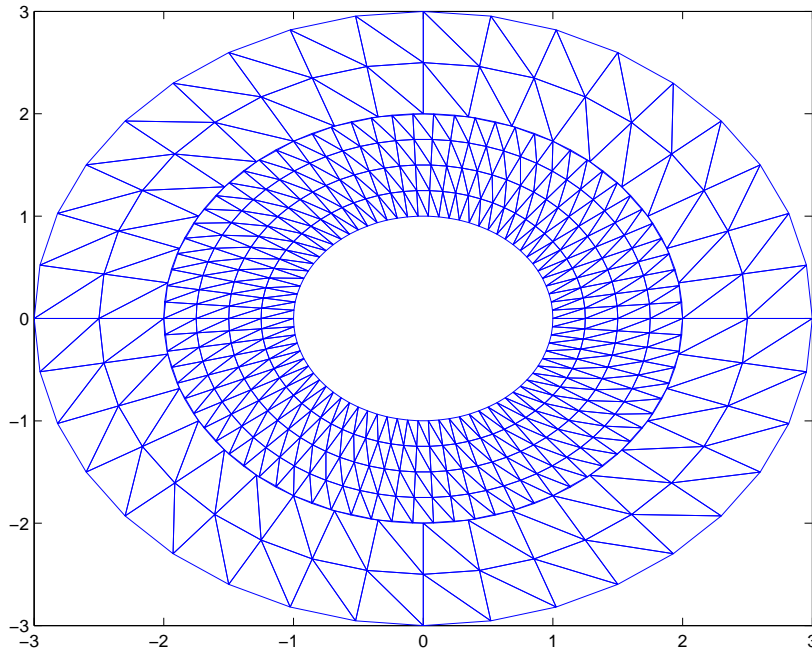


Figure 4: The uniform triangular division for Example 1

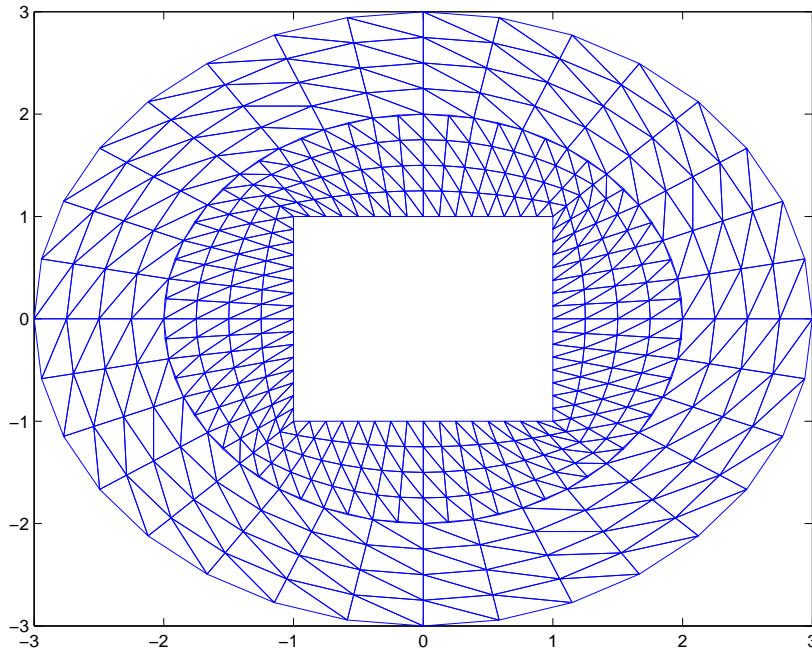


Figure 5: The uniform triangular division for Example 2

corresponding linear systems by the conjugate gradient method. In Table 1, the discretization errors are given in the L^2 -norm and energy norm as well as L^∞ -norm for the two subdomains, where $NEM1$ and $NEM2$ are the number of elements in $\Omega_i, i = 1, 2$, respectively. $iters$ indicates the number of iterations required by the D-N alternating method. Here we adopt the notation

$$\|u - u_{h_i}\|_{\infty, \Omega_i} := \max_{j \in \{1, \dots, NEMi\}} |u(x_j) - u_{h_j}(x_j)|, \quad i = 1, 2. \quad (5.3)$$

We observe that the energy error is of order h and the error in the L^2 -norm is of order h^2 . In Figure 6, the errors in the energy norm and the L^2 -norm are shown versus the number of elements, which also indicate that the errors are asymptotic optimal. The exact solutions and numerical solutions are visualized in Figure 9 and Figure 8.

Table 1: Comparison of errors for CG solvers.

$NEM1$	$NEM2$	$\ u_1 - u_{h_1}\ _{0, \Omega_1}$	Ratio	$\ u_1 - u_{h_1}\ _{1, \Omega_1}$	Ratio	$\ u_1 - u_{h_1}\ _{\infty, \Omega_1}$
64	16	1.3957×10^{-1}	—	8.9967×10^{-1}	—	4.0603×10^{-2}
256	64	3.7894×10^{-2}	3.683	4.5687×10^{-1}	1.969	8.9620×10^{-3}
1024	256	9.7081×10^{-3}	3.903	2.2980×10^{-1}	1.988	2.0970×10^{-3}
4096	1024	2.4428×10^{-3}	3.974	1.1510×10^{-1}	1.997	5.0595×10^{-4}
16384	4096	6.1171×10^{-4}	3.993	5.7574×10^{-2}	1.999	1.2403×10^{-4}
64512	16384	1.5902×10^{-4}	3.847	2.9207×10^{-2}	1.971	3.1644×10^{-5}
258043	64512	3.9781×10^{-5}	3.997	1.4604×10^{-2}	2.000	7.9193×10^{-6}

$\ u_2 - u_{h_2}\ _{0, \Omega_2}$	Ratio	$\ u_2 - u_{h_2}\ _{1, \Omega_2}$	Ratio	$\ u_2 - u_{h_2}\ _{\infty, \Omega_2}$	iters
1.2019×10^{-1}	—	4.4410×10^{-1}	—	6.1547×10^{-2}	11
3.0114×10^{-2}	3.783	2.1131×10^{-1}	2.007	1.6227×10^{-2}	11
7.4141×10^{-3}	3.860	1.0449×10^{-1}	1.996	3.3571×10^{-3}	11
1.8516×10^{-3}	3.916	5.2155×10^{-2}	1.998	7.2441×10^{-4}	12
4.6399×10^{-4}	4.004	2.6070×10^{-2}	1.999	1.9160×10^{-4}	12
1.2697×10^{-4}	3.836	1.3035×10^{-2}	2.000	4.8141×10^{-5}	13
6.4486×10^{-5}	3.290	6.5416×10^{-3}	1.984	1.2032×10^{-5}	13

Example 2. Let Ω_0 be a square with center at $(0, 0)$ and side lengths given by 1 (see Figure 5). The exact solution is given by

$$u_1(x, y) = \sin(\pi x) \sin(\pi y) \quad u_2(x, y) = \frac{x^2 - y^2}{(x^2 + y^2)^2} + \frac{x}{x^2 + y^2}. \quad (5.4)$$

Here we choose the matrix valued function as

$$A = \begin{pmatrix} \epsilon & 0 \\ 0 & 1 \end{pmatrix} \quad (5.5)$$

with

$$f(x, y) = (\epsilon + 1)\pi^2 \sin(\pi x) \sin(\pi y). \quad (5.6)$$

In Table 2, order h for the energy norm and the order h^2 for the L^2 -norm can be observed. The discretization errors are plotted in Figure 10.

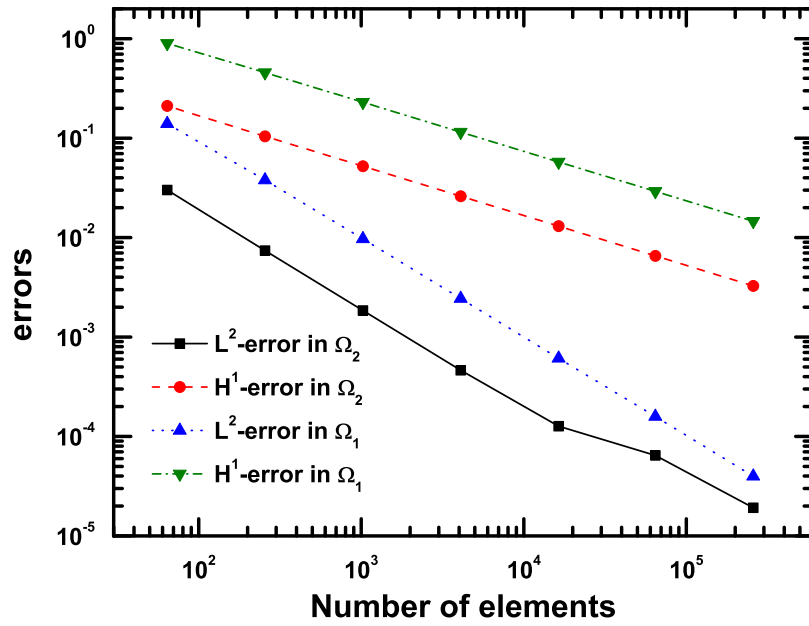


Figure 6: Discretization errors in L^2 -norm and H^1 -norm versus number of elements for Example 1.

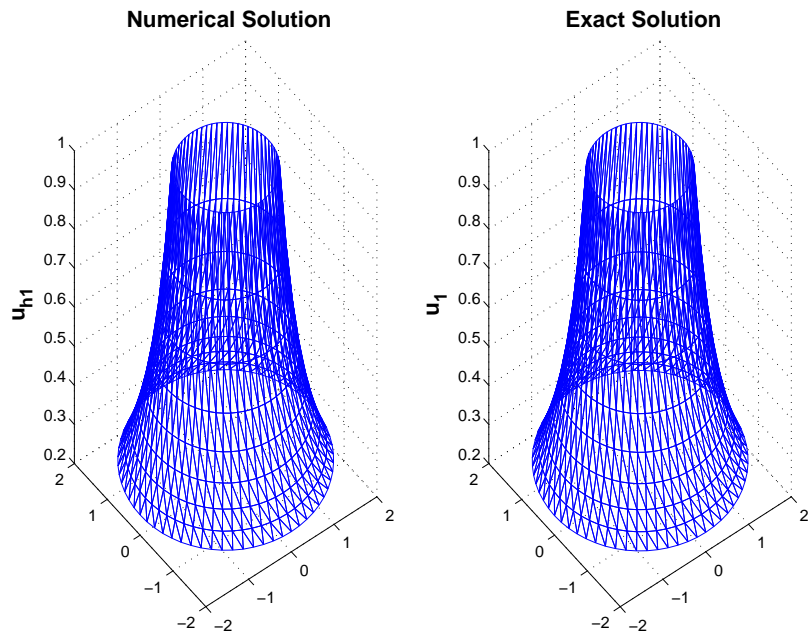


Figure 7: Finite element solutions in Ω_1 for example 1.

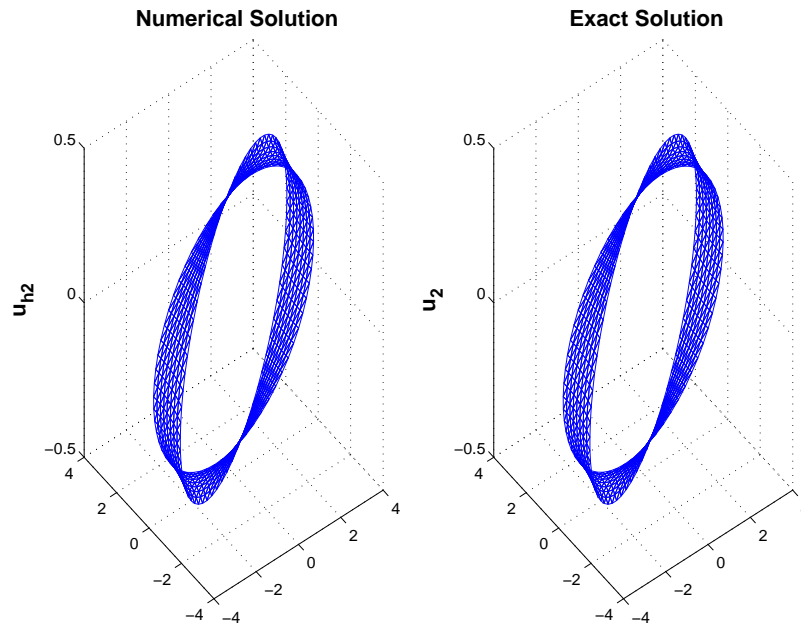


Figure 8: Finite element solutions in Ω_2 for example 1.

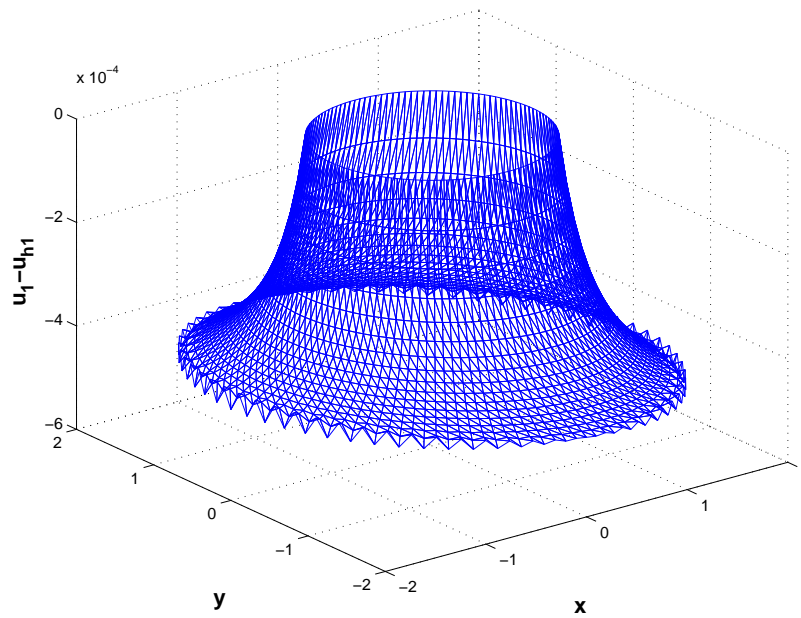


Figure 9: Finite element errors in Ω_1 for example 1.

Table 2: Comparison of errors for CG solvers.

$NEM1$	$NEM2$	$\ u_1 - u_{h_1}\ _{0,\Omega_1}$	Ratio	$\ u_1 - u_{h_1}\ _{1,\Omega_1}$	Ratio	$\ u_1 - u_{h_1}\ _{\infty,\Omega_1}$
64	16	6.8473×10^{-1}	—	4.18518	—	2.7447×10^{-1}
256	64	2.7053×10^{-1}	2.531	2.52416	1.658	1.6151×10^{-1}
1024	256	7.6572×10^{-2}	3.533	1.32712	1.902	3.0370×10^{-2}
4096	1024	1.9716×10^{-2}	3.884	0.67223	1.974	8.6012×10^{-3}
16384	4096	4.9566×10^{-3}	3.978	0.33723	1.993	2.2386×10^{-3}
64512	16384	1.2375×10^{-3}	4.005	0.16964	1.988	5.6412×10^{-4}
258043	64512	2.9445×10^{-4}	4.203	0.08484	2.000	1.4442×10^{-4}

$\ u_2 - u_{h_2}\ _{0,\Omega_2}$	Ratio	$\ u_2 - u_{h_2}\ _{1,\Omega_2}$	Ratio	$\ u_2 - u_{h_2}\ _{\infty,\Omega_2}$	iters
1.8424×10^{-1}	—	0.67003	—	6.1547×10^{-2}	11
5.1630×10^{-2}	3.568	0.34369	1.950	4.0774×10^{-2}	8
1.2182×10^{-2}	4.238	0.16975	2.025	8.9008×10^{-3}	9
3.0108×10^{-3}	4.046	0.08475	2.003	1.8041×10^{-3}	7
7.5245×10^{-4}	4.001	0.04238	2.000	4.2226×10^{-4}	7
1.9506×10^{-4}	3.858	0.02119	2.000	1.2427×10^{-4}	7
7.4485×10^{-5}	2.620	0.01064	1.992	5.5621×10^{-5}	7

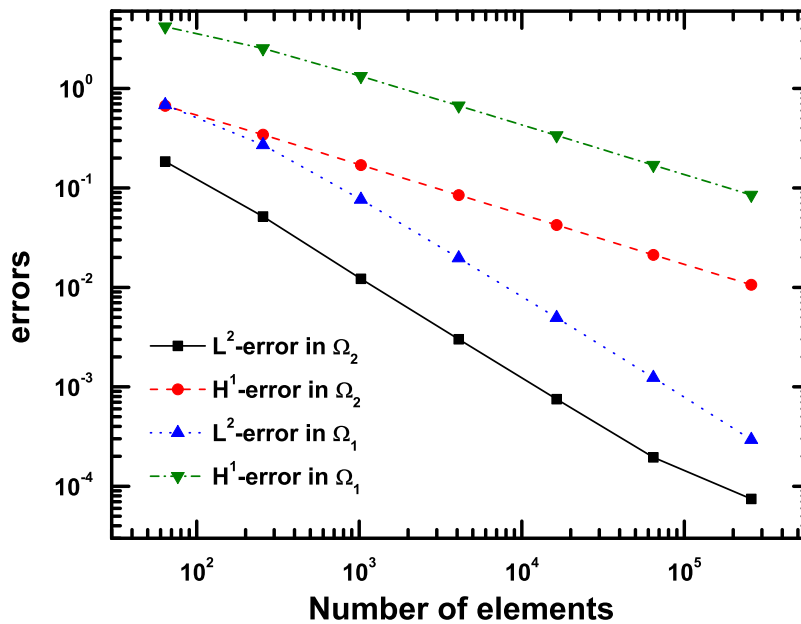


Figure 10: Discretization errors in L^2 -norm and H^1 -norm versus number of elements for Example 2.

References

- [1] F. Belgacem, The mortar element method with Lagrange multipliers, *Numer. Math.*, **84** (1999), 173-197.
- [2] C. Bernardi, Y. Maday and A. Patera, A new nonconforming approach to domain decomposition: the mortar element method, In: *Nonlinear partial differential equations and their applications. College de France Seminar, Vol. XI (Paris, 1989-1991)*, Longman Sci. Tech., Harlow, 1994, 13-51.
- [3] P. G. Ciarlet, *The finite element method for elliptic problems*, North-Holland, Amsterdam, 1978.
- [4] Qiya Hu, Zhongci Shi and Dehao Yu, Efficient solvers for saddle-point problems arising from domain decompositions with Lagrange multipliers, *SIAM J. Numer. Anal.*, **42:3** (2004), 905-933.
- [5] Qiya Hu, Numerical integrations and unit resolution multipliers for domain decomposition methods with nonmatching grids, to appear in *Computing*.
- [6] P. S. Vassilevski, T. Kolev, J. Pasciak, Algebraic Construction of Mortar Finite Element Spaces With Application to Parallel AMGe, 11th Copper Mountain Conference on Multigrid Methods (March 30-April 4), UCRL-JC-153326, Copper Mountain CO., 2003.
- [7] B. I. Wohlmuth, A mortar finite element method using dual spaces for the Lagrange multiplier, *SIAM J. Numer. Anal.* **38** (2000), 989-1012.
- [8] Ju'e Yang, Qiya Hu, Dehao Yu, Domain decomposition with non-matching grids for coupling of FEM and natural BEM, *J. Sys. Sci. Complex*, **18:4** (2005), 529-542.
- [9] Dehao Yu, The coupling of natural BEM and FEM for Stokes problem on unbounded domain. *Chinese J. of Numer. Math. and Appl.*, **14:4** (1992), 111-120.
- [10] Dehao Yu, *Mathematical Theory of Natural Boundary Element Method*, Science Press, Beijing, 1993.
- [11] Dehao Yu, *Natural Boundary Integral Method and Its Applications*, Science Press/Kluwer Academic Publishers, Beijing, 2002.